Photoelectrocatalytic decomposition of dye in aqueous solution using Nafion as an electrolyte

Wen-Yu Wang[a], Ming-Lun Yang[b], Young Ku[b],*

[a] Department of Environmental Engineering and Management, Chaoyang University of Technology, 168 Jifong E. Rd., Wufong Township, Taichung County, Taiwan
[b] Department of Chemical Engineering, National Taiwan University of Science and Technology, 43, Keelung Road, Section 4, Taipei 106, Taiwan

ABSTRACT

In this research, methylene blue (MB) was use as a pollutant to investigate the capability of dye degradation of photocatalytic (UV/TiO$_2$) and photoelectrocatalytic (UV/TiO$_2$/bias) reaction, and also the condition for UV/TiO$_2$/bias process was optimized. The photocatalytic process with bias potential was conducted in aqueous supporting electrolyte and with a proton exchange membrane (Nafion 117). Comparing with the general use of aqueous electrolyte (e.g. NaSO$_4$, KCl, or NaCl) in photoelectrocatalytic process, this study was focused on the application of proton exchange membrane as a solid electrolyte for the photoelectrocatalytic decomposition of MB. The degradation of MB was experimentally studied by a varied reaction condition (i.e. solution pH value, UV light intensity, initial dye concentration, gas introduction, supporting electrolyte concentration, and bias potential). Degradation of MB was enhanced in UV/TiO$_2$/bias process as compared to that carried out in UV/TiO$_2$ process, especially as the Nafion membrane was applied (UV/TiO$_2$/Nafion process). The photodegradation rates could also be boosted by increasing the concentration of supporting electrolyte, concentration of dissolving oxygen and UV light intensity. In UV/TiO$_2$/Nafion process, the rate constants of MB degradation increased as increasing bias potential to a certain level, and then it leveled off. The suitable bias potentials for experiments conducted at pH 5.3 and 7.0 were found to be 0.5 and 0.6 V, respectively.

© 2010 Elsevier B.V. All rights reserved.

1. Introduction

The performance of dye fixation represents an important fraction of the commercialized synthetic pigments used. The major environmental problem associated with the use of dyes is their loss in the dyeing process. Up to date, frequently the dye fixation efficiency is low; consequently, substantial amounts of unfixed dyes are released into the wastewater. The loss of dye during the dyeing process requires a proper treatment before discharged to the environment. The color and toxicity caused by dyestuffs may pose adverse impact on water quality, environment and human health [1]. At present, the most common technology for the removal of dyestuffs from aqueous solutions is chemical coagulation following by sedimentation, which generates a massive amount of sludge and induces further environment pollution. Therefore, the removal of dyestuffs from industrial wastewater has encouraged dynamic research activities in the development of several specialized treatment technologies [2,3].

Photocatalytic processes using TiO$_2$ as a catalyst have attracted extensive attention for various environmental applications to decompose organic contaminants into simple inorganic species [4].

This includes removal of dye pollutants from textile wastewater [5]. TiO$_2$ in anatase form is a promising photocatalyst because of its high chemical and photoelectrochemical durability, appropriate band-gap (3.0 eV) to adsorb UV-A light at 365 nm, and comparative inexpensiveness. The photocatalytic properties of TiO$_2$ particles have been investigated extensively in slurry and immobilized-film reactors [6–9]. However, the shortcoming of photocatalytic process is the rapid recombination of electron–hole pairs [5]. The oxidation and reduction reactions may occur on the same photocatalyst particle and a short-circuit electron transfer may occurred. This accelerated the recombination and lowered the removal efficiencies and quantum yield. For the reasons, several novel methods have been applied to increase the photocatalytic efficiencies. Rauf et al. [10] constructed a Cr–Ti binary oxide by sol–gel method and used it as photocatalyst to degrade methylene blue (MB) solution. Chen et al. [11] assembled a TiO$_2$ nanotube array by anodic oxidation method and treated MB solution with photocatalysis and photoelectrocatalysis. The synergetic effect of UV light and electric field showed a better result on the degradation of MB. By the application of external bias voltage [12–15] to photocatalytic process (called electrochemically assisted photocatalytic process or photoelectrocatalytic process), the photocatalyst acts as photoanode and an external anodic bias is applied to drive the photogenerated electrons and holes in opposing directions so that the charge recombination is retarded.

* Corresponding author. Tel.: +886 2 23785535; fax: +886 2 23785535.
  E-mail address: ku508@mail.ntust.edu.tw (Y. Ku).

In photoelectrocatalysis, the organic pollutants in the solution increase the cell resistance. In the presence of supporting electrolyte, this resistance is greatly reduced. The employment of electrolyte solution is important to the photocurrents as well as degradation efficiencies. Furthermore, the selection of electrolyte is also critical. The introduction of Nafion as a solid electrolyte was planned to simplify the addition of supporting electrolyte. Nafion 117 membrane is a well-known proton exchange membrane and is applied in fuel cell extensively, especially in PEMFC area. In fuel cell Nafion membrane could transfer proton (H^+) from anodic compartment to cathodic one and formed water. Nafion 117 membrane was used as a role of salt bridge in two-compartment reactor [16,17] to conduct the humic acid degradation and investigation of active chlorine, chlorate and bromate formation in photoelectrocatalysis.

This study investigated the capability of dye degradation by photoelectrocatalytic (UV/TiO$_2$/bias) reaction and a novel method that used a proton exchange membrane (Nafion 117) to replace the aqueous supporting electrolyte in solution. The impact of a varied reaction condition were examined including solution pH, UV light intensity, gas introduction, bias potential and supporting electrolyte, by this approach the study evaluated the application of Nafion 117 on dye degradation and optimized the reaction condition for the further application on industry.

2. Experimental

2.1. Ti mesh electrode

Ti mesh (>99.5%, 1.5 mm × 3.0 mm opening, President) was immersed in 0.5 N H_2SO_4 (>95%, Acros) to clean the oxide on the surface. Then it was rinsed with ethanol (95% C_2H_5OH, Osaka) and acetone for several times in order to remove the impurities and grease. TiO$_2$ particles were coated on a piece of Ti mesh of 20 mm × 50 mm by impregnating the mesh in an aqueous suspension containing TiO$_2$ and dioctylsulfosuccinate (99.9% $C_{20}H_{37}OSNa$, Sigma). Water to TiO$_2$ ratio in the aqueous suspension is 4:1 in weight. The impregnation and drying process could be repeated for several times to increase the amount of TiO$_2$ coated on the Ti mesh. Following the coating process, the electrode was put in a furnace (at 350 °C) for 1 h. Several coated meshes were made and weighed. Among them, three meshes with TiO$_2$ loading of 60 ± 2 mg were chosen to accomplish the UV/TiO$_2$, UV/TiO$_2$/bias, and UV/TiO$_2$/Nafion processes (described in the Section 2.3). Then the coated electrode was connected with a wire by means of silver adhesive. The counter electrode was made of stainless steel mesh (50 mesh, 0.297 mm opening). It was cut into the same size as anodic electrode, and rinsed with ethanol and acetone before being connected to a wire.

Nafion, an anionic perfluorinated polymer with sulfonate groups, is chemical, electronic, and photochemical inert. It is stable in dye aqueous solution whether the solution is acidic or alkaline. Nafion membrane was put into 3% H_2O_2 (35%, Acros) boiling solution (100 °C) for 40 min, and then into 9 M HCl (>35%, Osaka) boiling solution (80 °C) for 20–30 min. After rinsing with deionized water and cleaning by ultrasonication for 10 min, the membrane was boiled in deionized water for 30 min. Before the Nafion membrane was employed in the experiments, it was immersed into 30 mg L^{-1} MB aqueous solution. In UV/TiO$_2$/Nafion process, Nafion 117 membrane was placed between two electrodes to form a sandwich structure as shown in Fig. 1(a).

2.2. Photoreactor

The experiment was conducted using a batch photoreactor, UV lamp, and a pair of anode–cathode with applying Nafion film as
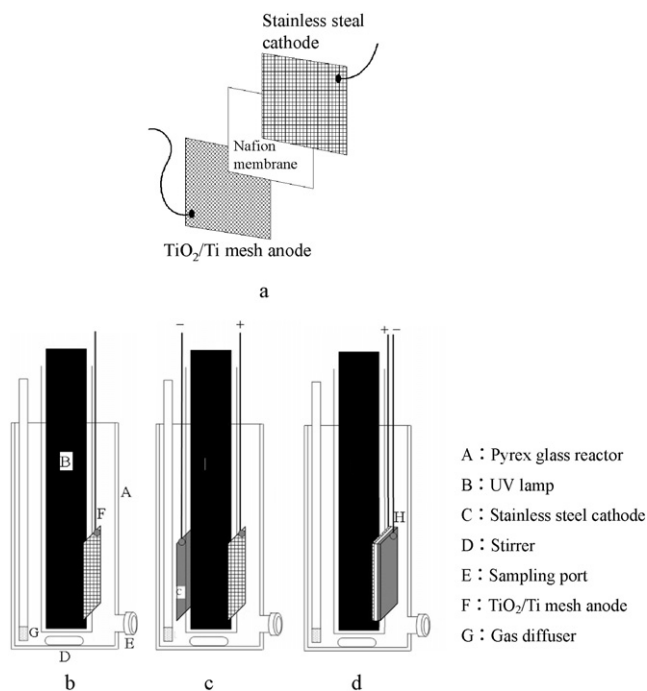

Fig. 1. (a) Schematic structure of electrodes employed in UV/TiO$_2$/bias process with Nafion, and scheme of reactor for (b) UV/TiO$_2$ process, (c) UV/TiO$_2$/bias process, and (d) UV/TiO$_2$/bias process with Nafion.

the supporting electrolyte as shown in Fig. 1. The cylinder photoreactor was made of Pyrex with an outer diameter of 63 mm, inner diameter 52 mm, height 225 mm, and sampling ports. The efficient volume of photoreactor was 220 mL after subtracting the volume occupied by the quartz jacket, and volume of MB solution introduced was 200 mL. The UV source is a 10 W blacklight lamp (UV-A, peak wavelength 365 nm). The UV light intensities were measured on blacklight lamp surface at a height of the middle of Ti mesh electrode by an International Light's IL1400 digital radiometer. The UV lamp protected by the quartz jacket from the bulk solution was put into the photoreactor in the duration of the reaction.

2.3. Photocatalysis and photoelectrocatalysis

The capability of MB degradation was tested by three processes, including UV/TiO$_2$ (Fig. 1(b)), UV/TiO$_2$/bias (Fig. 1(c)) and UV/TiO$_2$/Nafion processes (Fig. 1(d), Nafion used as a solid electrolyte in the UV/TiO$_2$/bias process). All the MB degradation processes were evaluated on the effect of solution pH, light intensity, and gas introduction from the diffuser (O$_2$, air, and N$_2$). The effect of bias voltage and supporting electrolyte as either Nafion or NaCl (0–100 mol m^{-3}) were investigated for the degradation using UV/TiO$_2$/bias and UV/TiO$_2$/Nafion processes. The effect of initial MB concentration was also studied. For experiments conducted under different conditions, reaction solution was sampled at predetermined time intervals from the reactor for the determination of MB by a Shimatsu UV-160A spectrophotometer. The absorbance wavelength used in the spectrophotometer analysis to determine MB concentration was 664 nm. A linear calibration line was obtained from 0.23 to 6.00 mg/L of MB. Therefore, all the samples were diluted 5 times before UV/vis absorption analysis.

3. Results and discussion

The effects of operational parameters such as: solution pH, light intensity, and gas introduction from the diffuser (O$_2$, air, and N$_2$)
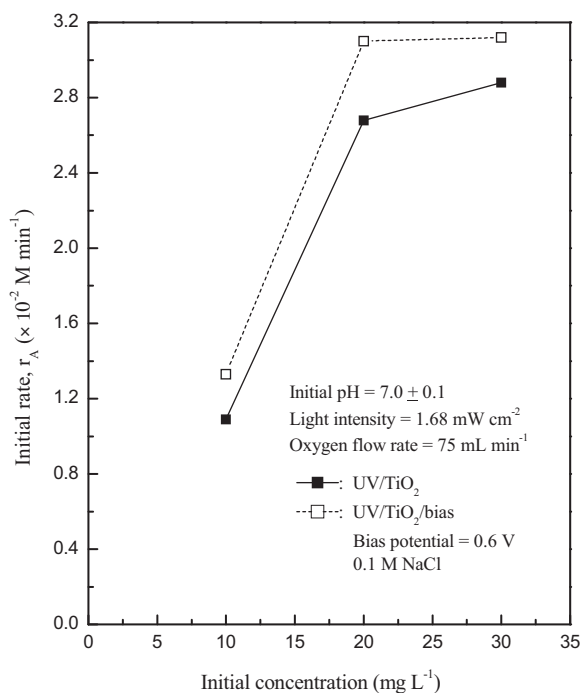
Fig. 2. Effect of initial concentration of dye on the initial reaction rate constants of UV/TiO$_2$ process and UV/TiO$_2$/bias process with the assistance of supporting electrolyte.

were examined using the reaction set in UV/TiO$_2$, UV/TiO$_2$/bias and UV/TiO$_2$/Nafion processes following the procedures described above.

It should be noted that experiments of each process were conducted in different electrodes. For example, the influences of solution pH on UV/TiO$_2$, UV/TiO$_2$/bias and UV/TiO$_2$/Nafion processes were conducted with three different plates of TiO$_2$ coated on the three Ti meshes. Even about the same weight $(60 \pm 2\,\text{mg})$ of TiO$_2$ was coated on the three Ti mesh. There may be various morphologies among different electrodes because the TiO$_2$ particles coated on the Ti mesh were identical but not have equal extent of coverage on Ti mesh. Consequently, it should not put emphasis on the comparison between processes and only the tendencies of each process were discussed.

3.1. Effect of initial methylene blue concentration

The rate constant for the photocatalytic degradation was calculated from experimental data using the well-known Langmuir–Hinshelwood equation (L–H equation). Generally, the reaction rates increase with an increase in substrate concentration of a chemical reaction. Langmuir–Hinshelwood model (L–H model) was applied to describe the photocatalytic reaction behavior. The equation is as follows:

$$r_A = -\frac{dC_A}{dt} = \frac{kKC_A}{1 + KC_A} \qquad (1)$$

In photocatalytic reaction, the initial concentrations of MB were designed to be 10, 20, and 30 mg L^{-1} and pH value and light intensity was 7.0 and 1.68 mW cm^{-2}, respectively. As shown in Fig. 2, the initial reaction rate conducted with initial concentration of 20 mg L^{-1} was more than twice of that conducted with 10 mg L^{-1}. However, the initial rate did not increase much as we expected when the initial concentration was 30 mg L^{-1}, and it seemed to level off in further high initial concentrations no matter in UV/TiO$_2$ or UV/TiO$_2$/bias process. The initial concentration of 30 mg L^{-1} was significant corresponding to the TiO$_2$ loading of 6 mg cm^{-2}. Espe-

cially in weak alkaline solution, the MB adsorption on TiO$_2$/Ti mesh electrode was obviously high. It was observed that too high surface coverage would result in a decrease in degradation rates.

Lakshmi et al. [18] reported that the initial reaction rates increased linearly during initial MB concentrations of 6.6–20.0 μM in a photocatalytic suspension reactor. Then, the initial rates leveled off as the MB concentrations were over 20.0 μM. Sivalingam et al. [19] studied the photocatalytic degradation of MB aqueous solution with various initial concentrations (50–200 mg L^{-1}) in suspension reactor. The TiO$_2$ dosage was designed to be 1.0 g L^{-1} in this set of experiments. It can be seen that the concentration had a significant effect on the degradation rates and the rate of decrease in the MB concentration is faster when the initial concentration was low. The degradation rates were lower for higher initial concentrations as the order decreases and, therefore, the Langmuir–Hinshelwood rate equation was proposed to model the experimental data. The initial reaction rates increased with an increase in initial MB concentrations and leveled off at higher concentrations. Adsorption and surface reaction were assumed to be the rate controlling steps and these parameters were determined using Langmuir–Hinshelwood rate equation. In brief, the reaction order over concentration ranged from zero to unity in photocatalytic process as well as photoelectrocatalytic process.

Although dye solution can be decolorized completely by photocatalytic or photoelectrocatalytic process, it must be mentioned that complete decoloration does not mean complete mineralization in photocatalytic or photoelectrocatalytic process. Spectroscopic analysis only measures color removal but complete mineralization must be evidenced by the total organic carbon concentrations. The major goal of photocatalytic process is elimination of parent compound, or more specifically, detoxification of an inhibitory and/or persistent pollutant [20], but in some reactions the intermediate oxidation products remaining in the solution may be as toxic as or even more toxic than the initial compound [21].

As shown in Fig. 2, the initial rates in UV/TiO$_2$/bias were faster than that in UV/TiO$_2$ process. In the electrochemical perspective, the oxidation and reduction reaction occurred on the same TiO$_2$ particle at the same time and then formed a short circuit in photocatalytic reaction. Due to recombination, the electrons and holes were very easy to disappear. The application of bias potential was the most special feature in UV/TiO$_2$/bias process. An electric field would be established between anode and cathode with the bias potential applied. By applying an electrochemical bias potential to a TiO$_2$ membrane, separation of photogenerated electrons and holes was accelerated and the recombination of electrons and holes was suppressed. At the same time, photoexcited electrons could be withdrawn to a counter electrode through an external circuit. The oxidation and reduction reaction might occur in different electrodes, and the overall reaction rates and quantum efficiencies might be enhanced.

The coulombic efficiency of the process is still not significant. We suggest that a small ratio of surface area of the TiO$_2$/Ti mesh to MB solution volume (1:20) brings about a low contribution of coulombic effect. Other reason is a too large space between the anode and cathode, a diameter of 52 mm of quartz protected jacket for UV lamp, and a shield effect of electric field by the quartz protected jacket. Introduction of oxygen also promotes the reaction efficiency of UV/TiO$_2$ process without external bias.

3.2. Effect of solution pH

Solution pH values played an important role in many chemical reactions. In the case of TiO$_2$ photocatalyst, the surface binding states were changed with pH [22]. TiO$_2$ existed in the form of –TiOH in aqueous solution. However, the states would change to either TiOH$_2^+$ or TiO$^-$ based on the adsorption, dissociation behavior, and
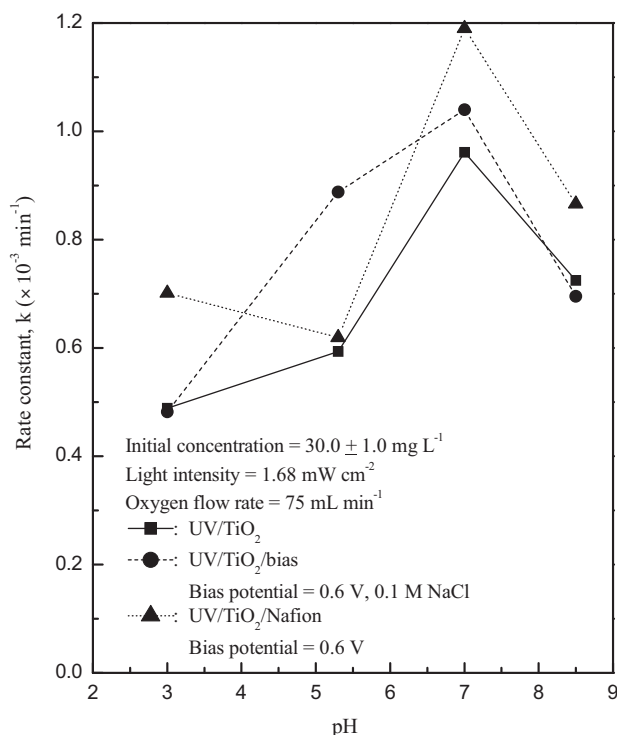
Fig. 3. Effect of pH on the pseudo-first-order reaction rate constants of UV/TiO$_2$ process and UV/TiO$_2$/bias process with the assistance of supporting electrolyte or Nafion membrane.

solution compositions. It also changed surface charges of TiO$_2$ particles and resulted in a significant electrostatic interaction between species in the aqueous solution. Some researchers inferred that the probability of production of hydroxyl free radicals was raised in alkaline aqueous solution which is rich in hydroxyl ions. The indirect oxidation might dominate the photocatalytic reaction in alkaline solution. Nevertheless, the surface reaction was complicated in several interactions in the same time. The pH settings in photocatalytic reaction were controlled within a range from 3.0 to 8.5. According to the results of background experiments, it was possible for MB to react with OH$^-$ at solution pH over 9. In order to avoid it, the present experiments only conducted at weak alkaline solution.

The photocatalytic reaction was controlled strongly by solution pH because of the electrostatic force. The results of pH effect are shown in Fig. 3. The removal rate constants were increased with an increase in solution pH as pH values were less than 7.0. The rate constant reduced to a lower level at pH 8.5 but was still higher than that obtained at pH 3.0 and 5.3. The reaction rates had strong dissociation with the adsorption of MB molecules on TiO$_2$ membrane. The adsorption behaviors were influenced extensively by solution pH. Dyestuff MB had an acid dissociation constant (pK_a) below 0 [23] so it would be positively charged in aqueous solution at all the times. The zero point of charge of TiO$_2$ suspension and membrane were measured to be 6.8 and 6.5, respectively [24]. The TiO$_2$ surface was positively charged and would repel with positively charged MB molecules as long as pH was lower than 6.5. In contrast, the two species would attract each other in neutral and alkaline solution.

When the solution pH was adjusted to be 3.0, the adsorption was weaker than that of experiments conducted in higher pH values. This was proved in the adsorption experiments and was indicated by Houas et al. [25] and Hasnat et al. [26]. Hasnat et al. studied the adsorption of MB at pH range 4.0–10.0 and found that the MB adsorption increased with an increase in solution pH. Electrostatic interactions between the negatively charged TiO$_2$ particles and MB

cations led to strong absorption and enhanced the degradation rate.

When the experiment was conducted at pH 8.5, both the efficiency and rate constant were found to be lower than that obtained at pH 7.0. The reaction at neutral condition had great removal efficiency as well as reaction rate constant. The phenomenon might be attributed to critically high adsorption on TiO$_2$ surface at pH 8.5. The amount of TiO$_2$ particles coated on Ti mesh electrode (10 cm^2) was only 60 mg, which meant that the available active site was limited, and catalytic reaction would be a rate-limiting step of overall reaction rate as the quantity of MB adsorption was too high. It may shelter from the illumination of incident UV light. Lakshmi et al. [18] investigated that the photocatalytic degradation of MB solution by suspension system. The conditions were designed to be initial concentration of 0.01 mM of MB solution and TiO$_2$ dosage of 20 mg in 75 mL reactor. The reaction is found to conform to a Langmuir adsorption isotherm and the rate vs. pH profile exhibits a linear increase with pH in acidic solutions with a maximum at around pH 6.9.

As shown in Fig. 3, no matter in UV/TiO$_2$, or UV/TiO$_2$/bias process the pseudo-first-order reaction rate constants were highest at pH 7.0, and then at pH 5.3 or 8.5, and the worst at pH 3.0. With Nafion applied in UV/TiO$_2$/bias process, a higher rate constant was obtained from experiment conducted at pH 3.0 compared with that obtained at pH 5.3. This could be explained to the concentrated hydrogen ions at pH 3.0 induced better proton exchange ability. As the aqueous electrolyte (NaCl) was replaced by solid electrolyte (Nafion 117 membrane), the performances were not improved much.

3.3. Effect of light intensity

From the background experiments of adsorption equilibrium, it was found that the catalytic reaction did not occur without UV light illumination. The light intensity has influence not only on the progress of the photocatalytic reaction but also on the extent of electron–hole pairs generated. Additionally, the UV light decay in air or solution was described by Beer–Lamber law (Beer's law).

$$A = \varepsilon bc \tag{2}$$

where A is the absorbance at certain wavelength; ε the molar absorptivity, cm^{-1} M^{-1}; b the path length of the sample, cm; and c is the concentration of the compound in solution, M.

The data of molar absorptivity of MB were calculated from the calibration lines, which were measured by UV/vis spectrophotometer. The molar absorptivity of MB was 6.0×10^4 cm^{-1} M^{-1}. Because the molar absorptivity of MB was high, the high adsorption on TiO$_2$/Ti mesh electrode might induce the shelter effect of emitting UV light.

The investigated UV light intensities were set from 0.83 to 1.68 mW cm^{-2}. The solution was adjusted to pH 7.0 and oxygen was introduced. The initial concentration was controlled to be 30 mg L^{-1}. Fig. 4 reveals that the pseudo-first-order reaction rate constants increased linearly with an increase in light intensities. With the UV light intensity increased, the separation rate of electron–hole pairs were accelerated and resulted in increasing of the production of hydroxyl free radicals as well as the degradation rate constants and removal efficiencies. Zhang et al. [27] studied the degradation of MB by UV/TiO$_2$ process in a suspension reactor. The results revealed that the linear dependence of the apparent rate constants on light irradiance with light intensity ranged from 0.98 to 7.20 mW cm^{-2}.

In UV/TiO$_2$/bias process, the application of bias potential and concentration of supporting electrolyte were fixed to be 0.6 V and 0.10 M NaCl, respectively. The pseudo-first-order reaction rate constants are shown as a function of light intensity in Fig. 3. The
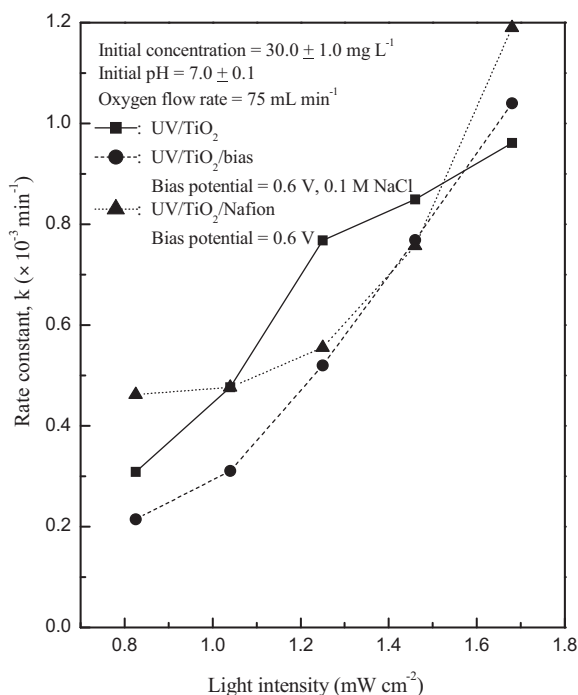
Fig. 4. Effect of light intensity on the pseudo-first-order reaction rate constants of UV/TiO$_2$ process and UV/TiO$_2$/bias process with the assistance of supporting electrolyte or Nafion membrane.

Fig. 5. Effect of oxygen content of gas introduced on the pseudo-first-order reaction rate constants of UV/TiO$_2$ process and UV/TiO$_2$/bias process with the assistance of supporting electrolyte or Nafion membrane.

tendency was linear as the light intensity ranged from 1.04 to 1.68 mW cm^{-2}.

As shown in Fig. 4, in the application of Nafion membrane in UV/TiO$_2$/bias process (i.e. UV/TiO$_2$/Nafion process) the rate constants were increased with an increase in light intensity, but somewhere different from that observed in experiments conducted with aqueous electrolyte employed. The rate constants were improved little by increasing the light intensity when the light intensities were relatively low. The rate constant of experiment conducted with light intensity of 1.68 mW cm^{-2} was 150% higher than that of experiment conducted with light intensity of 0.83 mW cm^{-2}.

The improvement of increasing light intensity was insignificant in UV/TiO$_2$/Nafion process as the light intensities were relatively low. In the configuration of UV/TiO$_2$ and UV/TiO$_2$/bias processes, the TiO$_2$/Ti mesh electrode was pressed close to the quartz jacket. The MB decay in solution should be neglected. Nevertheless, the TiO$_2$/Ti mesh electrode would have a distance of 4 mm with the quartz jacket because of the space between quartz jacket and electrode clamps. When the sandwich form electrode was immersed into MB solution, this space would be filled with MB solution, too. A shelter effect of emitting UV light should happen in the course of UV/TiO$_2$/Nafion process and caused the different results between the experiments with and without Nafion membrane. Comparing with UV/TiO$_2$/bias and UV/TiO$_2$/Nafion process, the UV/TiO$_2$ process performs a comparable MB degradation ratio with different reaction parameters. As mentioned in Section 2.1, three different meshes were chosen to accomplish the UV/TiO$_2$, UV/TiO$_2$/bias, and UV/TiO$_2$/Nafion processes, respectively. There may be some variations beside catalyst weight (e.g. surface morphologies or profiles) among the three meshes.

3.4. Effect of oxygen introduction

In photocatalytic oxidation process, the photogenerated electrons are driven away and avoided from recombination with holes.
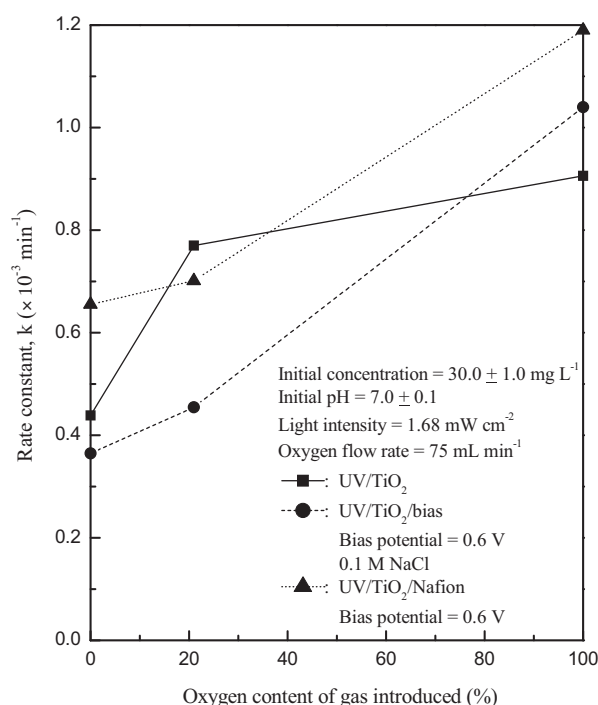
The most extensive and convenient solution is to purge oxygen, which will trap the electrons to form peroxide radicals. If the solution was purged with nitrogen or argon, the accumulated electrons on TiO$_2$ surface would accelerate the electron–hole recombination and reduce the removal efficiency. Therefore, dissolved oxygen in aqueous solution has significant influence in photocatalytic process. In the view of hydroxyl free radical formation, the hydroxyl free radicals generated from holes or hydrogen peroxide. Since the hydrogen peroxide was formed from oxygen, the high level of dissolved oxygen in aqueous solution would promote the generation of hydroxyl radicals further.

The experiments were conducted with oxygen (100% O$_2$), air (21% O$_2$), and nitrogen (0% O$_2$) introduction. As shown in Fig. 5, the rate constant of UV/TiO$_2$ process conducted with air introduction was 75% higher than that with nitrogen introduction. However, the enhancement of oxygen introduction was not evident compared with that of air introduction, but onefold higher than that of nitrogen introduction. The removal efficiency of experiment conducted with nitrogen introduction was only somewhat higher than that of photolysis reaction. More electron scavenger (O$_2$) in aqueous solution would reduce the recombination rate. Thus, increasing the dissolved oxygen concentration would also increase the reaction rate constants in UV/TiO$_2$ and UV/TiO$_2$/bias processes.

The removal efficiencies increased with an increase in dissolved oxygen concentration in reaction solution. Briefly, the removal efficiencies would be promoted by oxygen introduction, then air and nitrogen introduction. As shown in Fig. 5, the tendencies were fitted well in each process. The rate constants increased with an increase in oxygen contents of gas introduced into the reaction solution. An interesting phenomenon in photocatalytic degradation of MB was reported by Mills and Wang [28]. MB was indeed bleached, and formed a significant amount of MB(H$_2$)$^+$, since with the subsequent introduction of oxygen into the system the MB was regenerated. The recovery of the MB, with the introduction of oxygen, was ca. 63–68%. It appeared that such radicals were the cause for the extensive (32–37%) irreversible photobleaching. The rate of reaction of
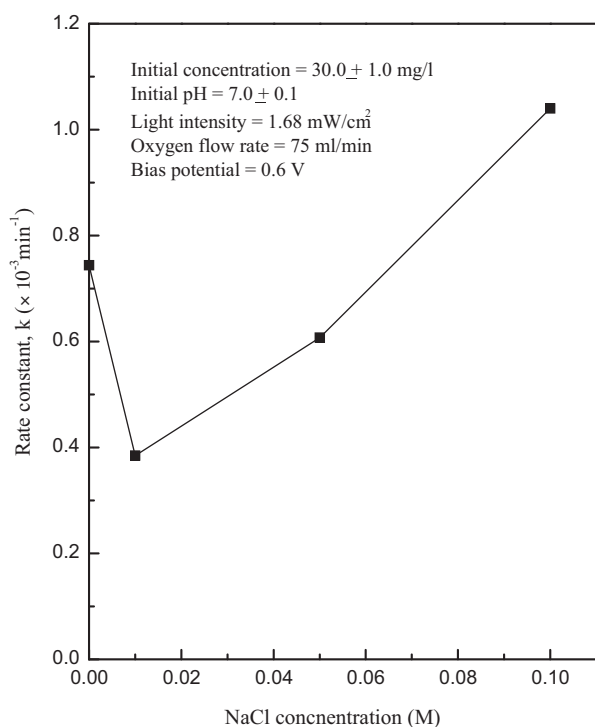
Fig. 6. Effect of sodium chloride addition on the pseudo-first-order reaction rate constants for the decomposition of methylene blue by UV/TiO$_2$/bias processes.

Fig. 7. Effect of supporting electrolyte addition on the removal percentages for the decomposition of methylene blue by various processes.

MB recovery was strongly dependent upon the level of oxygen present. The rate appeared to be dependent directly on the percentage of O$_2$ present in the purging gas stream at levels <60%, but became increasingly insensitive to any increase in percentage of O$_2$ above a level of 60. Gas-to-liquid mass transfer would be expected to become the rate determining step.

3.5. Effect of supporting electrolyte

The category and concentration of aqueous supporting electrolyte were most frequently studied factors in UV/TiO$_2$/bias process. The existence of aqueous electrolyte might alter the reaction mechanism and either enhances or reduces the reaction efficiencies. Supporting electrolyte in aqueous solution could also lower the ohmic resistance. The selection of supporting electrolyte should be paid more attention at the stage of reaction designation. Generally, the supporting electrolyte would be inorganic salts, such as carbonates, chlorides, nitrates, sulfates and so on. Some electrolytes could react with the model pollutants directly without further treatment via photocatalytic process. For example, the MB solution would react with perchlorate (ClO$_4^-$) ion and formed a violet precipitate if perchlorate salt or perchloric acid was chosen as an aqueous electrolyte. Although many studies reported that the perchlorate salt was one of the most electrochemically stable electrolytes in photoelectrocatalytic process, it did not suit for every treated contaminant.

Fig. 6 shows the rate constants in the UV/TiO$_2$/bias process were 7.44×10^{-4}, 3.85×10^{-4}, 6.07×10^{-4} and 10.4×10^{-4} min^{-1} in 0, 0.01, 0.05 and 0.10 M NaCl solution, respectively. The rate constant drops clearly with 0.01 M NaCl addition compared with that conducted with no addition of supporting electrolyte. Then, the rate constants would increase with an increase in supporting electrolyte concentration. The removal efficiency obtained from the experiment conducted with electrolyte concentration of 0.10 M was higher than that obtained from the experiment conducted without supporting electrolyte addition. The reason may be that the
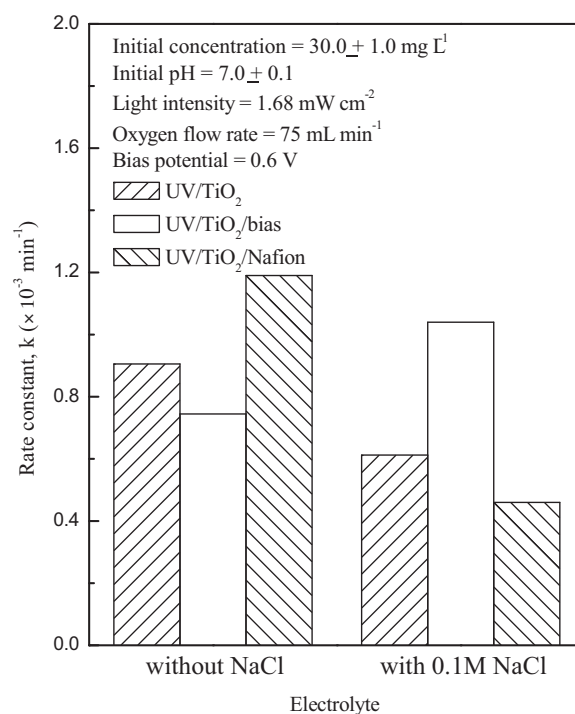
chloride ions would capture the photogenerated holes [24]. However, the rates of degradation and the amount degraded increased as the concentrations of NaCl increased from 0.01 to 0.10 M. This may be attributed to higher reduction in ohmic resistance in aqueous MB solution. Zainal et al. [29] achieved similar results and reported further that a higher concentration, 0.25 M NaCl, resulted in only a slight increase in the degradation. Addition of supporting electrolytes such as Na$_2$CO$_3$ and Na$_2$SO$_4$ results in a slight decrease in photodegradation of the R3R dye in comparison with that carried out in an electrolyte free system in NaOH [30]. The addition of NaClO$_4$ slightly decreased the photoelectrocatalytic removal efficiency of oxalic acid [31].

Fig. 7 shows the influence of aqueous supporting electrolyte addition on each process. In both UV/TiO$_2$ and UV/TiO$_2$/Nafion processes, the addition of supporting electrolyte did not promote the removal efficiency and had negative effects. In UV/TiO$_2$ process, the chloride ions would capture the photogenerated holes. In UV/TiO$_2$/Nafion process, the high amount of sodium ions would be incorporated into Nafion membrane. Okada et al. [32] and Unnikrishnan et al. [33] reported that the Nafion film was converted into Na$^+$ form by equilibrating the membrane in the acid form with excess of 0.10 M NaCl solution for 5 h followed by repeated washing with deionized water. From the results, the membrane prefers Na$^+$ to H$^+$ and in the corresponding membrane H$^+$ moves about five times faster than Na$^+$ ions. The water transference coefficient in Nafion was much larger for Na$^+$ form than that of H$^+$ form, in spite of the smaller equilibrium water content for Na$^+$ form than for H$^+$ form.

Only in UV/TiO$_2$/bias process, the addition of supporting electrolyte had a positive effect. Furthermore, it can be noticed that the addition of 0.10 M NaCl would result in an increase in removal efficiency. It may be attributed to the strong improvement in conductivity of the solution by 0.10 M NaCl addition could balance the negative effect of hole competition. In addition, the chloride ions may react with photogenerated holes and form chloride radicals, chlorate, and chlorine. It can be observed that the variation of
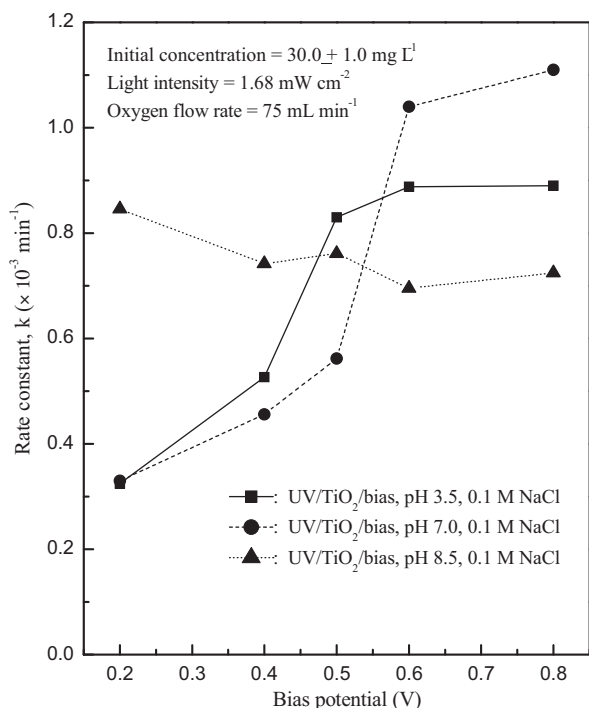
Fig. 8. Effect of bias potential on the pseudo-first-order reaction rate constants of UV/TiO$_2$/bias process at pH 3.5, 7.0 and 8.5.

Fig. 9. Effect of bias potential on the pseudo-first-order reaction rate constants of UV/TiO$_2$/bias and UV/TiO$_2$/Nafion processes at pH 7.0.

chloride ions concentration was within 6% by means of the measurement of ion chromatography. This implied that the extent of reaction between chloride ion and hole was insignificant.

3.6. Effect of bias potential

In the electrochemical perspective, the oxidation and reduction reaction occurred on the same TiO$_2$ particle at the same time and then formed a short circuit in photocatalytic reaction. The electrons and holes were very easy to disappear due to recombination. The application of bias potential was the most special feature in UV/TiO$_2$ process. An electric field would be established between anode and cathode with the bias potential applied. By applying an electrochemical bias potential to a TiO$_2$ film, separation of photogenerated electrons and holes was accelerated and the recombination of electrons and holes was suppressed. At the same time, photoexcited electrons could be withdrawn to a counter electrode through an external circuit. The oxidation and reduction reaction might occur in different electrodes, and the overall reaction rates and quantum efficiencies might be enhanced. If the bias potential applied was not high enough, the promotion would be limited and even no improvement at all. In contrary, high bias potential would induce electrolysis of water. The anode, TiO$_2$ thin film, would be destroyed because of the formation of oxygen when the water electrolysis occurred.

The photoelectrocatalytic degradation of MB was conducted with light intensity of 1.68 mW cm^{-2} and oxygen introduction. Bias potentials applied were set to be 0.2, 0.4, 0.5, 0.6, and 0.8 V. 0.10 M NaCl solution and Nafion membrane were taken as a supporting electrolyte in UV/TiO$_2$/bias and UV/TiO$_2$/Nafion processes, respectively. As shown in Fig. 8, the pseudo-first-order reaction rate constants increased as the bias potentials increased from 0.2 to 0.6 V at pH 3.5 and 7.0. Then, the rate constant increased a little as the bias potential applied was 0.8 V. It is reasonable to say that the efficiency would level off in higher bias potential as long as the water electrolysis takes place. However, this incremental tendency did not arise when the experiments were carried out at pH 8.5 and
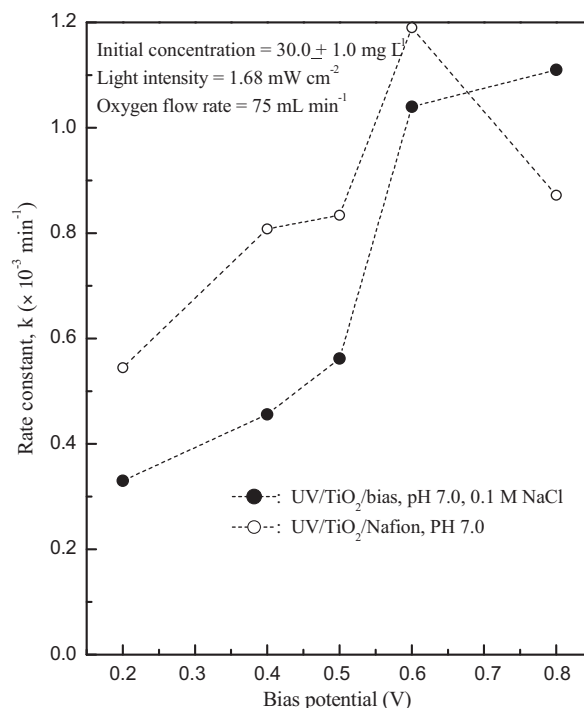
the rate constants were almost equal in all bias potentials applied.

Fig. 9 shows the effect of bias potential on the pseudo-first-order reaction rate constants of UV/TiO$_2$/bias and UV/TiO$_2$/Nafion processes at pH 7.0. In UV/TiO$_2$/Nafion process with Nafion applied, the rate constants increased with an increase in bias potentials applied besides that obtained from experiment conducted with bias potential of 0.8 V. The best performance was found to be with the experiment conducted with a bias potential of 0.6 V. Nafion 117 membrane, which was taken as solid electrolyte, was employed to photoelectrocatalytic reaction in order to replace the additional usage of aqueous supporting electrolyte. In addition, the MB solution was free from aqueous supporting electrolyte (to improve the conductivity of the photoelectrocatalytic system, but the photocatalytic properties was inhibited by the scavenging of hydroxyl radicals by ions). The close contact between two electrodes and Nafion membrane was a great benefit to reduce the ohmic resistance. The protons diffused rapidly through the sulfonate-form microscopic channels in Nafion directly without diffusion in aqueous solution. Another advantage of employment of solid electrolyte, Nafion, was that the electrochemical reactions between anion of electrolyte and photocatalyst could be avoided.

4. Conclusion

Photocatalytic and photoelectrocatalytic reactions of MB demonstrated a pseudo-first-order reaction. The photocatalytic reaction was controlled strongly by solution pH because of the electrostatic force. The best removal efficiencies occurred at pH 7.0. High light intensity could provide more protons and correspondingly more electron–hole pairs and promote reaction rate. The reaction rate constants increased with an increase in dissolved oxygen concentration and UV light intensity because more electron scavengers (oxygen) in aqueous solution slow down the electron–hole recombination process.

Degradation of MB was promoted in UV/TiO$_2$/bias process. Applying bias potential to drive away electrons and minimizing the electron–hole recombination, thus the reaction rate constants can

be increased. In UV/TiO$_2$/bias process, reaction rates were accelerated by increasing of supporting electrolyte that enhanced the conductivity of MB solution. A linear relationship was obtained between rate constants and concentrations of supporting electrolyte. In UV/TiO$_2$/bias process, the rate constants increased as increasing bias potential to a certain level, and then it leveled off.

Comparing with traditionally aqueous electrolyte, Using Nafion as a solid electrolyte shows a comparable efficiency in photoelectrocatalytic process. In the past, it was difficult to apply photoeletrocatalytic process in waste gas treatment because of no electrolyte as electric media in gas stream. The sandwich structure of cathode-Nafion-photoanode used in this study provides another possible application area in pollution treatment.

References

[1] K.T. Fletcher, Design the environment and textiles: developing strategies for environmental impact reduction, J. Text. I. 89 (1998) 72–80.
[2] T. Robinson, G. McMullan, R. Marchant, P. Nigam, Remediation of dyes in textile effluent: a critical review on current treatment technologies with a proposed alternative, Bioresour. Technol. 77 (2001) 247–255.
[3] H. Ma, Q.F. Zhuo, B. Wang, Electro-catalytic degradation of methylene blue wastewater assisted by Fe$_2$O$_3$-modified kaolin, Chem. Eng. J. 155 (1–2) (2009) 248–253.
[4] M.R. Hoffmann, S.T. Martin, W. Choi, Environmental application of semiconductor photocatalysis, Chem. Rev. 95 (1995) 69–96.
[5] W. Baran, E. Adamek, A. Makowski, The influence of selected parameters on the photocatalytic degradation of azo-dyes in the presence of TiO$_2$ aqueous suspension, Chem. Eng. J. 145 (2) (2008) 242–248.
[6] D.F. Ollis, Contaminant degradation in water, Environ. Sci. Technol. 19 (1985) 480–484.
[7] I. Sopyan, M. Watanabe, S. Murasawa, An efficient TiO$_2$ thin-film photocatalyst: photocatalytic properties in gas-phase acetaldehyde degradation, J. Photochem. Photobiol. A 98 (1996) 79–86.
[8] W.Y. Wang, Y. Ku, Photocatalytic degradation of Reactive Red 22 in aqueous solution by UV-LED radiation, Water Res. 40 (2006) 2249–2258.
[9] W.Y. Wang, A. Irawan, Y. Ku, Photocatalytic degradation of Acid Red 4 using a titanium dioxide membrane supported on a porous ceramic tube, Water Res. 42 (2008) 4725–4732.
[10] M.A. Rauf, M.A. Meetani, A. Khaleel, A. Ahmed, Photocatalytic degradation of methylene blue using a mixed catalyst and product analysis by LC/MS, Chem. Eng. J. 157 (2–3) (2010) 373–378.
[11] Y. Chen, L.Y. Shi, S. Yuan, J. Wu, M.H. Zhang, J.H. Fang, Photoelectrocatalytic degradation of methylene blue by TiO$_2$ nanotube array prepared by anodic oxidation, J. Inorg. Mater. 24 (4) (2009) 680–684.
[12] C.C. Sun, T.C. Chou, Kinetics and mechanism of photoelectrochemical oxidation of nitrite ion by using the rutile form of a TiO$_2$/Ti photoelectrode with high electric field enhancement, Ind. Eng. Chem. Res. 37 (1998) 4207–4214.
[13] C.C. Sun, T.C. Chou, Electrochemically promoted photocatalytic oxidation of nitrite ion by using rutile form of TiO$_2$/Ti electrode, J. Mol. Catal. A—Chem. 151 (2000) 133–145.
[14] X.Z. Li, H.L. Liu, P.T. Yue, Y.P. Sun, Photoelectrocatalytic oxidation of Rose Bengal in aqueous solution using a TiO$_2$/Ti mesh electrode, Environ. Sci. Technol. 34 (2000) 4401–4406.
[15] K.W. Kim, E.H. Lee, Y.J. Kim, M.H. Lee, D.W. Shin, A study on characteristics of an electrolytic–photocatalytic reactor using an anode coated with TiO$_2$, J. Photochem. Photobiol. A 161 (2003) 11–20.
[16] H. Selcuk, J.J. Sene, M.A. Anderson, Photoelectrocatalytic humic acid degradation kinetics and effect of pH, applied potential and inorganic ions, J. Chem. Technol. Biotechnol. 78 (2003) 979–984.
[17] H. Selcuk, M.A. Anderson, Effect of pH, charge separation and oxygen concentration in photoelectrocatalytic system: active chlorine production and chlorate formation, Desalination 176 (2005) 219–227.
[18] S. Lakshmi, R. Renganathan, S. Fujita, Study on TiO$_2$-mediate photocatalytic degradation of methylene blue, J. Photochem. Photobiol. A 88 (1995) 163–167.
[19] G. Sivalingam, K. Nagaveni, M.S. Hegde, G. Madras, Photocatalytic degradation of various dyes by combustion synthesized nano anatase TiO$_2$, Appl. Catal. B—Environ. 45 (2003) 23–38.
[20] I. Arslan-Alaton, Degradation of a commercial textile biocide with advanced oxidation processes and ozone, J. Environ. Manage. 82 (2007) 145–154.
[21] R. Munter, Advanced oxidation processes—current status and prospects, Proc. Estonian Acad. Sci. Chem. 50 (2001) 59–80.
[22] C. Kormann, D.W. Bahnemann, M.R. Hoffmann, Photolysis of chloroform and other organic molecules in aqueous TiO$_2$ suspensions, Environ. Sci. Technol. 25 (1991) 494–500.
[23] A.R. Disanto, J.G. Wagner, Pharmacokinetics of highly ionized drugs. II. Methylene blue—absorption, metabolism, and excretion in man and dog after oral administration, J. Pharm. Sci. 61 (1972) 1086–1090.
[24] W.Y. Wang, Y. Ku, Effects of solution pH and UV irradiation on the streaming potential of the titanium dioxide membranes, J. Membr. Sci. 282 (2006) 342–350.
[25] A. Houas, H. Lachheb, M. Ksibi, E. Elaloui, C. Guillard, J.M. Herrmann, Photocatalytic degradation pathway of methylene blue in water, Appl. Catal. B—Environ. 31 (2001) 145–157.
[26] M.A. Hasnat, I.A. Siddiquey, A. Nuruddin, Comparative photocatalytic studies of degradation of a cationic and an anionic dye, Dyes Pigments 66 (2005) 185–188.
[27] T. Zhang, T. Oyama, A. Aoshima, H. Hidaka, J. Zhao, N. Serpone, Photooxidative N-demethylation of methylene blue in aqueous TiO$_2$ dispersions under UV irradiation, J. Photochem. Photobiol. A 140 (2001) 163–172.
[28] A. Mills, J. Wang, Photobleaching of methylene blue sensitised by TiO$_2$: an ambiguous system? J. Photochem. Photobiol. A 127 (1999) 123–134.
[29] Z. Zainal, C.Y. Lee, M.Z. Hussein, A. Kassim, N.A. Yusof, Effect of supporting electrolytes in electrochemically-assisted photodegradation of an azo dye, J. Photochem. Photobiol. A 172 (2005) 316–321.
[30] P.A. Carneiro, M.E. Osugi, J.J. Sene, M.A. Anderson, M.V.B. Zanoni, Evaluation of color removal and degradation of a reactive textile azo dye on nanoporous TiO$_2$ thin-film electrodes, Electrochim. Acta 49 (2004) 3807–3820.
[31] T. An, G. Li, X. Zhu, J. Fu, G. Sheng, Z. Kun, Photoelectrocatalytic degradation of oxalic acid in aqueous phase with a novel three-dimensional electrode-hollow quartz tube, Appl. Catal. A—Gen. 279 (2005) 247–256.
[32] T. Okada, S. Møller-Holst, O. Gorseth, S. Kjelstrup, Transport and equilibrium properties of Nafion membranes with H$^+$ and Na$^+$ ions, J. Electroanal. Chem. 442 (1998) 137–145.
[33] E.K. Unnikrishnan, S.D. Kumar, B. Maiti, Permeation of inorganic anions through Nafion ionomer membrane, J. Membr. Sci. 137 (1997) 133–137.